Engineering and Technology Journal
Journal homepage: https://etj.uotechnology.edu.iq

Investigation of machining performance in ecdm of Al6061-SiC-B_4C hybrid composites

Safa M. Lafta*, **Abbas F. Ibrahim**

Production Engineering and Metallurgy Dept., University of Technology-Iraq, Alsina'a street, 10066 Baghdad, Iraq.
*Corresponding author Email: pme.20.88@grad.uotechnology.edu.iq

HIGHLIGHTS

- ECDM for Al6061-SiC-B_4C composites was optimized using Taguchi analysis and ANOVA to enhance machining performance.
- 34% efficiency, 21% surface quality improvement at 20% electrolyte, 40 V, 150µs Pon.
- MRR and SR were improved, benefiting machining applications in aerospace, automotive, and defense industries.

Keywords:

Electrochemical Discharge Machining

Hybrid composite machining

Aluminum 6061

Silicon carbide

Boron carbide

ABSTRACT

This study investigates the machining performance of the Electrochemical Discharge Machining (ECDM) process on a hybrid composite material comprising Aluminum 6061 reinforced with 6% silicon carbide (SiC) and 6% boron carbide (B_4C). Experiments evaluated the effects of electrolyte concentration, voltage, pulse-on time, and pulse-off time on Material Removal Rate (MRR), Tool Wear Rate (TWR), and Surface Roughness (SR). Taguchi analysis and ANOVA highlighted the significant influence of these parameters on machining outcomes. The optimal MRR (0.113 g/min) was achieved at 20% electrolyte concentration, 40 V, 150 µs pulse-on time, and 25 µs pulse-off time. The best TWR (0.007 g/min) occurred at 30% concentration, 30 V, 150 µs pulse-on time, and 50 µs pulse-off time. The optimal SR (4.757 µm) was observed at 20% concentration, 30 V, 100 µs pulse-on time, and 75 µs pulse-off time. The findings emphasize the importance of parameter optimization in improving machining efficiency and surface integrity, offering valuable insights for hybrid composite applications. In particular, the study reveals that higher electrolyte concentrations and voltages generally enhance MRR but can increase TWR and degrade SR. These findings underline the importance of parameter optimization for balancing productivity and surface integrity. This research provides valuable insights for industries seeking precise and efficient machining of hybrid composites, showcasing a 34% enhancement in machining efficiency and a 21% improvement in surface quality using the optimized ECDM conditions.

1. Introduction

The increased utilization of micro-scale products in various scientific and technological fields has led to significant advancements in manufacturing methods. In this regard, traditional techniques such as electrochemical machining (ECM) and electric discharge machining (EDM) are primarily suitable for electrically conductive materials. In contrast, non-conductive materials require specialized setups that limit their applicability. This limitation has driven the development of hybrid methods to manufacture micro-scale products regardless of material conductivity and strength. To this end, electrochemical discharge machining (ECDM), which combines ECM and EDM, was introduced to address these challenges [1]. Composite materials, defined as combinations of two or more constituents with distinct physical and chemical properties, offer unique characteristics unattainable in individual materials [2]. These materials typically consist of a matrix phase reinforced by other materials. When the matrix is metallic and includes multiple reinforcement materials, the result is a hybrid metal matrix composite (HMMC). In particular, HMMCs are increasingly used in advanced engineering applications, including aerospace, automotive, defense, and nuclear industries, due to their high specific strength and hardness. However, machining HMMCs poses significant challenges for conventional methods due to their high reinforcement content. Therefore, non-traditional machining methods have become essential for processing these materials. Specifically, aluminum-based HMMCs, known for their enhanced hardness, wear resistance, and low thermal expansion, are widely studied. Particularly, reinforcements, such as silicon carbide (SiC), boron carbide (B_4C), and aluminum oxide (Al_2O_3), improve mechanical and tribological properties but make machining more

http://doi.org/10.30684/etj.2025.156592.1881
Received 12 January 2025; Received in revised form 11 February 2025; Accepted 28 February 2025; Available online 24 March 2025
2412-0758/University of Technology-Iraq, Baghdad, Iraq

demanding [3–8]. In this regard, several studies have investigated the effects of the machining parameters on the material removal rate (MRR) and the surface quality (SR) for HMMCs. For instance, Yan et al. [9], studied the influence of the process parameters on high SiC-content composites. While increasing the pulse-on time (Ton) enhanced the MRR, excessive pulse-off time (Toff) and high wire tension led to reduced efficiency and surface irregularities. Abbas et al. [10], optimized electrolyte concentration, voltage, and inter-electrode gap using Taguchi methods, highlighting a trade-off between increased MRR and surface quality degradation by using the electrochemical machine (ECM), and also found that higher energy discharge improves MRR in hybrid composites by using electrical discharge machining (EDM) [11]. Moreover, Gugulothu et al. [12], studied the effects of various (ECM) parameters on the MRR of a hybrid metal matrix composite comprising an aluminum alloy reinforced with fly ash and silicon carbide. However, it showed a slight decrease with the increase in electrolyte concentration. In particular, the study underscored the importance of optimizing the machining parameters to enhance the material removal efficiency in hybrid composites. Additionally, Mandal et al. [13], investigated the effects of voltage, duty cycle, and electrolyte concentration on the MRR and the SR using micro-ECDM (μ-ECDM) and powder-mixed ECDM (PMECDM). The results showed that PMECDM significantly enhanced the MRR and reduced the SR compared to μ-ECDM. They also demonstrated that adding Al_2O_3 powder to the electrolyte improved the MRR and reduced short-circuit problems. However, the process increased the operational complexity [14]. Selvarasu et al. [15], optimized EDM parameters for AZ61/7.5% B_4C nano-composites, achieving 81% MRR, 55% EWR, and 47% SR improvement with nano SiC mixed EDM oil compared to kerosene and EDM oil alone. Satyanarayana Dusanapudi et al. [16], studied the enhancing die-sinking EDM processes for hybrid metal matrix composites. It optimizes parameters like pulse-on time and peak current to improve material removal rate (MRR), tool wear rate (TWR), and surface roughness (SR). Using stir-cast composites. Mohankumar et al. [17], optimized EDM parameters for Al7075/B_4C composites using the Taguchi method, achieving optimal values of 0.5628 mm^3/min MRR, 0.0048 mm^3/min TWR, and 4.4034 μm SR. Higher current and Ton increased MRR, TWR, and SR. Arif et al. [18], developed and validated a thermal model for EDM of hybrid aluminum composites and optimized machining parameters experimentally. It highlighted the effects of pulse current, pulse-on time, and SiC nano-particles on machining performance, revealing optimal conditions and critical parameter influences. Limitations include dependency on specific materials and constraints. Arunachalam et al. [19], investigated the influence of EDM parameters on a magnesium-based hybrid composite (AZ31alloy with 5% MoS_2 and 5% B_4C). It enhanced machining efficiency, wear resistance, and hardness through powder metallurgy. The study revealed optimal EDM parameters for improved material removal rate (MRR) and tool wear rate (TWR), emphasizing the composite's low density and high durability. Mohankumar et al. [20], focused on optimizing EDM parameters for a hybrid aluminum metal matrix composite (Al7075 with 6% SiC and 6% B_4C). Using hybrid optimization techniques like Taguchi, EWM, TOPSIS, and GRA, it achieves improvements in MRR, EWR, and SR, validated through ANOVA and SEM analysis. Key findings include a 15% enhancement in closeness coefficients and a 16% improvement in Grey relational grades.This previous research shows the predominant focus on improving the MRR without sufficiently addressing the surface quality, with limited exploration of multi-parameter optimization for both the MRR and the SR.There was inadequate scalability and generalization of findings to other materials or machining setups.To handle these issues, the current research seeks to overcome some of the identified gaps but acknowledges certain limitations. The objectives include establishing precise interrelations between multiple machining parameters (e.g., voltage, electrolyte concentration) and their combined effects on surface integrity, generalizing the results to a broader spectrum of HMMCs with varying reinforcement properties, and verifying the optimized parameters across diverse operational environments. Particularly, this study aims to develop a comprehensive framework for optimizing the ECDM parameters to achieve balanced MRR and SR in machining HMMCs. Moreover, the study investigates the influence of the process variables on machining performance to address the limitations in previous studies. The study also proposes practical solutions to improve machining efficiency and surface quality in challenging composite materials. The aerospace, automotive, and military industries can benefit from the exceptional strength and wear resistance of Hybrid Metal Matrix Composites (HMMCs), such as aluminum 6061 reinforced with SiC and B_4C. These composites are difficult to machine, though, and need settings that are tuned for both efficiency and surface quality. This work attempts to achieve the best possible balance between material removal rate (MRR), tool wear rate (TWR), and surface roughness (SR) by optimizing ECDM settings for machining Al6061-SiC-B_4C composites. The objectives are to establish exact relationships between machining parameters and validate outcomes under various circumstances. The effects of electrolyte concentration (10%-30%), voltage (30 V-50 V), pulse-on time (50-150 μs), and pulse-off time (25-75 μs) on MRR, TWR, and SR were investigated through experiments utilizing a copper electrode and NaCl electrolyte. Taguchi analysis and ANOVA were employed to determine the ideal machining settings and statistically confirm the results. This research makes ECDM a feasible option for processing high-hardness hybrid composites in a range of industrial applications by improving machining efficiency while preserving surface quality.

2. Experimental work

2.1 Workpiece

This study uses a hybrid composite material of the Al6061 alloy reinforced with 6% wt silicon carbide (SiC) and 6% wt boron carbide (B_4C). The chemical compositions of the base material and the hybrid composite were analyzed to ensure proper material characterization. Table 1 presents the chemical composition of the Al6061 alloy, highlighting the key elements and their respective weight percentages. This table provides a baseline understanding of the elemental distribution in the base material. In addition, Table 2 illustrates the chemical composition of the Al6061-6%SiC-6%B_4C hybrid composite as determined by the Energy Dispersive X-ray Spectroscopy (EDX). The EDX results reflect a localized measurement near the

interface rather than a bulk composition analysis. This ensures an accurate interpretation of the data and acknowledges the spatial variation in elemental distribution. Particularly, the table details the atomic and weight percentages of the elements in the composite, confirming the incorporation of reinforcements (SiC and B_4C) into the aluminum matrix. These chemical composition analyses of the materials were conducted at the Al-Khoura company in Baghdad.

Table 1: Chemical Composition of Al6061

Element	Weight%	Element	Weight%
Si%	0.620	Ni%	0.0055
Fe%	0.117	Zn%	0.0030
Cu%	<0.300	Ti%	0.0106
Mn%	0.0009	V%	0.0165
Mg%	1.11	Al%	Bal.
Cr%	0.0353		

The chemical composition was analyzed at Al-Khoura company, and the balance percentage of Al confirms the primary composition of the alloy.

Table 2: Chemical Composition of Al6061-6%SiC-6%B_4C

Element	Atomic%	Weight%
B	38.8	22.1
C	9.9	6.2
O	2.6	2.2
Al	48.2	68.6
Si	0.5	0.8

2.1.1 The Stir-casting process

The stir-casting technique was employed to fabricate the hybrid composite material because it effectively achieves a uniform distribution of reinforcements within the metal matrix. Specifically, the Al6061 alloy was melted in a graphite crucible and heated to a temperature of 700 °C. Next, the molten aluminum was stirred using a mechanical stirrer at a speed of 500 rpm for 10 minutes. During stirring, silicon carbide (SiC) and boron carbide (B_4C) powders, each constituting 6% of the composite by weight, were gradually added to the molten alloy. In this regard, the stirring process ensured homogeneous dispersion of the reinforcement particles throughout the matrix. After proper stirring, the molten composite was poured into a steel mold with dimensions of 50 mm in length and 30 mm in diameter. After that, the cast material was allowed to cool naturally at room temperature to solidify. Next, the solidified castings were machined into the required dimensions using a milling machine for further analysis and experimentation. Figure 1 shows the stir casting process by portable drilling at 500 rpm.

Figure 1: The stir-casting process

In particular, the properties of the MMCs strongly depend on the strength of the interfacial bonding of the reinforcement and the matrix phase [21]. Figure 2 shows the specimens before and after machining after cutting them into the desired dimensions of 5 mm and 30 mm in thickness and diameter, respectively. Table 3 shows the particulars of SiC and B_4C particulates [22]. The silicon carbide (SiC) and boron carbide (B_4C) reinforcements used in this study were characterized using EDX to confirm the elemental composition. The EDX analysis was conducted at Al-Khoura company. The results shown in

Table 4 and Table 5 indicate the elemental distribution of SiC and B_4C, respectively. Figure 3 and Figure 4 show the SEM images of SiC and B_4C, respectively, showing particle distribution and grain size measurements.

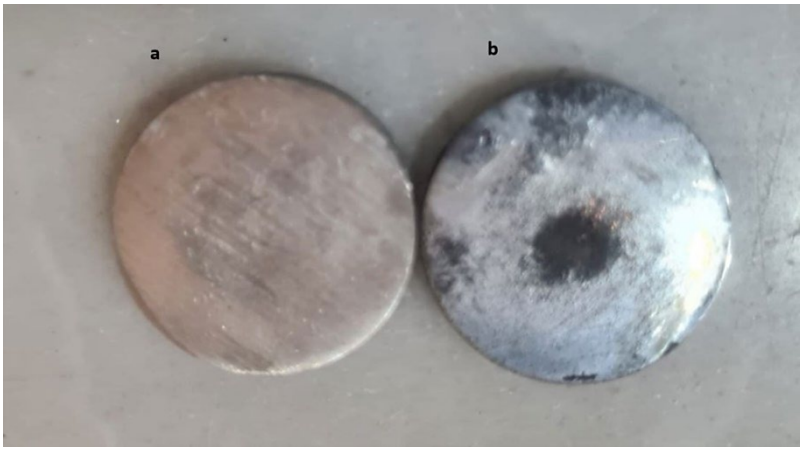

Figure 2: (a)The workpiece before machining and (b) after machining

Table 3: The particulars of SiC and B_4C particulates [22]

Reinforcement	Mean particle Size (µm)	Hardness (Kg/mm²)	Density (g/cm³)	Melting point (ºC)
SiC	35	2800	3.20	2700
B_4C	35	2450	2.52	2450

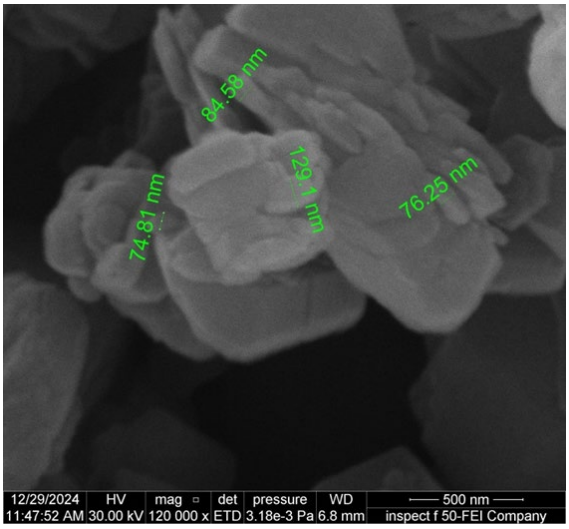

Figure 3: Distribution and grain size of SiC

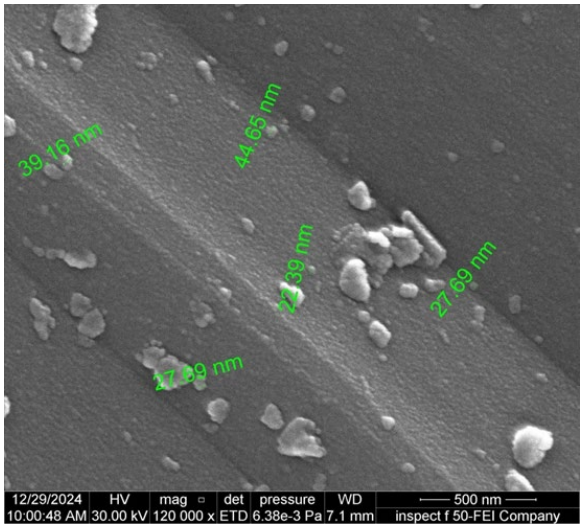

Figure 4: Distribution and grain size of B_4C

Table 4: Chemical Composition of SiC reinforcement particles

Element	Atomic%	Atomic% Error	Weight%	Weight% Error
C	38.9	0.9	24.9	0.5
O	25.6	0.5	21.8	0.4
Si	35.5	0.1	53.2	0.2

Table 5: Chemical Composition of B_4C reinforcement particles

Element	Atomic%	Atomic% Error	Weight%	Weight% Error
B	92.2	1.7	87.7	1.6
O	6.5	0.7	9.1	1.0
Si	1.3	0.1	3.2	0.2

The EDX analysis of SiC reinforcement confirmed the presence of silicon (35.5 %) and carbon (38.9%), which are the primary elements in silicon carbide. The detection of oxygen (25.6%) suggests surface oxidation, which is a common

occurrence in high-energy electron interactions during EDX analysis. These results confirm the successful incorporation of SiC as a reinforcing phase in the composite material; both powders (SiC and B_4C) originate from China Xi'an Function Material Group Co., Ltd., China. The purity for both was ≥ 99%, and particle size D 50= 40-46 µm.

The EDX analysis of B_4C reinforcement confirmed a high boron content (92.2%), which is characteristic of boron carbide. The presence of oxygen (6.5%) suggests minor surface oxidation, which is common in exposed surfaces analyzed via EDX. The minor detection of silicon (1.3%) may be attributed to trace impurities. These findings validate the successful incorporation of B_4C into the composite structure. Figure 5 shows the X-ray diffraction (XRD) for the specimen made of hybrid composite material Al-6%SiC-6%B_4C. The XRD analysis of Al-6%SiC-6%B_4C confirms a hexagonal crystal structure with distinct phases of aluminum, boron, silicon, and carbon. The strong diffraction peaks at 2θ ≈ 17.5°, 28.0°, and 37.6° indicate high crystallinity and phase stability. The presence of boron-silicon-carbon interactions suggests enhanced thermal stability, mechanical strength, and potential applications in high-performance ceramics, refractory materials, and electronic components.

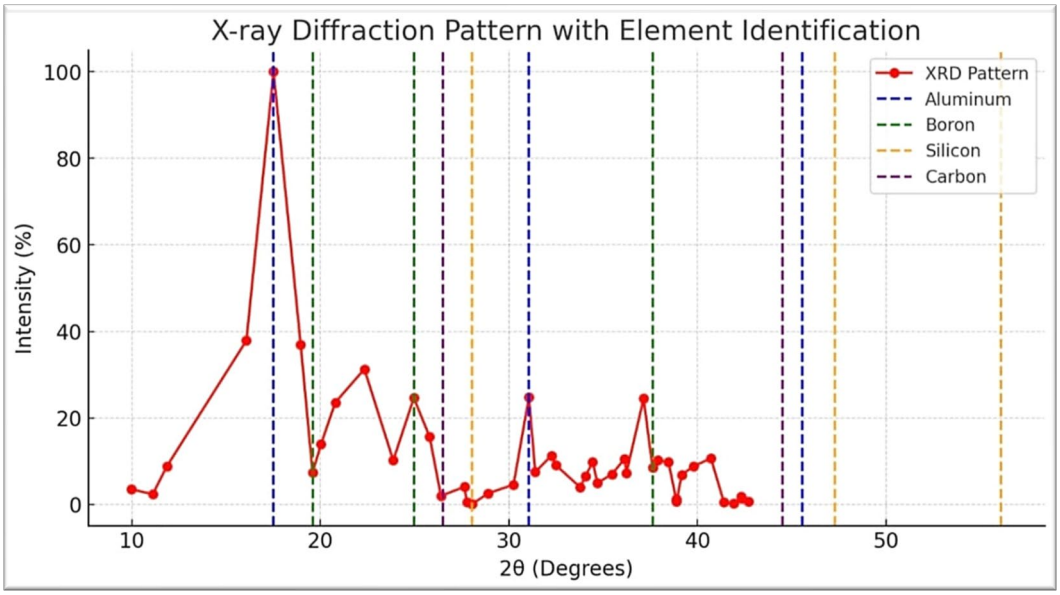

Figure 5: XRD for Al-6%SiC-6%B_4C

2.1.2 Tests and inspections

The Scanning Electron Microscope (SEM) was used to examine the microstructure of the prepared cast specimens of the composites, namely Al 6061 with 6% SiC and 6% B_4C. The wet grinding operation was made using SiC water and emery paper in various grits of 320, 500, 600, 800, 1000, and 1200. Particularly, the process of polishing was made on the samples using 0.5 µm diamond paste and special cloth for polishing and lubrication. Then, the etching process was carried out on the specimens utilizing the etching solution Keller's reagent (composed of 95 ml H_2O, 2.5 ml HNO_3, 1.5 ml HCL, and 1.0 ml HF). Figure 6 shows the base alloy Aluminum6061 with the distribution of particles (SiC and B_4C).

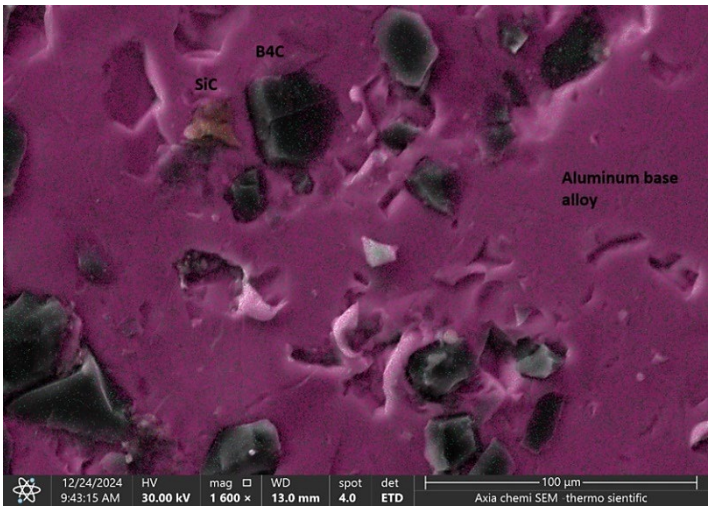

Figure 6: The distribution of particles at the aluminum base alloy

2.2 The Electrode

The copper electrode was used in the machining process as a cylindrical shape with dimensions of 50 cm and 10 mm in length and diameter, respectively. Specifically, a copper electrode was selected because of its high conductivity in both electrical and thermal properties, its ease of machining, and its high melting point of 1083 ℃, which is the most effective factor on tool wear. The tool was cleaned by washing it in water and dried after every process to remove the sludge that stuck on it. The physical properties of the copper electrode are shown in Table 6 [23], and Table 7 shows the chemical compositions of the copper electrode were analyzed at the state company for inspection and engineering rehabilitation SIER.

Table 6: The thermo-physical properties of the copper electrode [23]

Property	Value
Melting point	1083 ℃
Density	8.93 g/cm³
Thermal expansion coefficient	$16.4\times10^{-6}K^{-1}$
Thermal conductivity	385 W/m.K
Electrical resistivity	1.7×10^{-8} Ω.m

Table 7: The chemical composition of the copper electrode

Element	Weight%
Zn	0.0038
Pb	0.0011
Sn	0.0025
P	0.0007
Fe	0.0482
Cr	0.0008
Sb	0.0121
As	0.0007
Al	0.0152
S	0.0013
Cu	Bal.

2.3 Electrochemical discharge machining (ECDM)

Figure 7 shows the ECDM components.The ECDM was used to machine the hybrid composite material of Al6061 with 6% wt SiC and 6% wt B_4C because it is easy to machine complicated materials [24-28]. Specifically, the ECDM components include an acrylic tank, a power supply, and a computer system. The NaCl was used as an electrolyte. The operational setup involves the workpiece as the anode and the tool as the cathode.

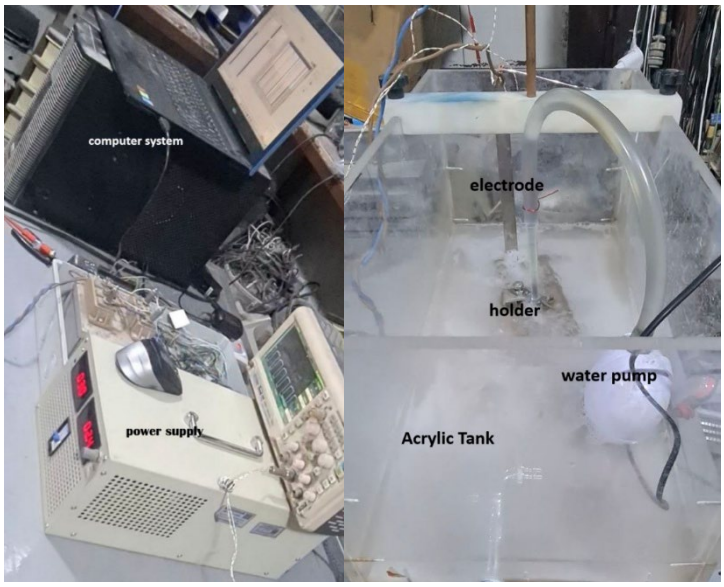

Figure 7: The ECDM components

The workpiece and the electrode were cleaned before each experiment and then cleaned of contaminants before the weighing process. Then, the workpiece was placed in a stainless-steel holder. The gap between the tool and the workpiece was 0.2 mm.

3. Results and discussion

After machining as shown in Equation 1, the MRR is determined by dividing the weight of the workpiece before and after the machining-on-machining time that was achieved [29].

$$MRR = (Wpb - Wpa)/MT \quad (1)$$

where MRR is the material removal rate (g/min), Wpb is the weight of the workpiece before machining (g), and Wpa is the weight of the workpiece after machining (g), and MT is the machining time (min), which was fixed in all the experiments (3 min).

After machining as shown in Equation 2, the tool wear rate (TWR) is determined by dividing the tool's weight before and after the machining-on-machining time that was achieved [30].

$$TWR = Eb - Ea/MT \quad (2)$$

where TWR is the tool wear rate (g/min), and Eb is the weight of the tool before machining (g), and Ea is the weight of the tool after machining (g), and MT is the machining time (min).

The SR was measured by a portable gauge of surface roughness from Mahr Federals in the Production Engineering and Metallurgy Department at the University of Technology. The experiments were conducted using NaCl electrolyte solution at three different concentrations (10%, 20%, and 30%). The applied voltage was varied at three levels: 30 V, 40 V, and 50 V. The pulse-on time (Pon) was set at 50 µs, 100 µs, and 150 µs, while the pulse-off time (Toff) was adjusted to 25 µs, 50 µs, and 75 µs. These parameters were selected based on prior studies and optimized to achieve the best machining performance. Table 8 shows the input parameters.

Table 8: The input parameters

Parameters	Symbols	Levels		
		1	2	3
Concentrations % (Con.%)	X1	10%	20%	30%
Voltages (V)	X2	30	40	50
Pulse on time (µsec) (Pon)	X3	50	100	150
Pulse off time (µsec) (Poff)	X4	25	50	75

In this study, the Taguchi array design L9 (3^4) was selected to efficiently analyze the effects of four parameters (electrolyte concentration, voltage, pulse-on time, and pulse-off time) at three levels. The L9 design was chosen instead of L81 to minimize the number of experiments while still maintaining statistical reliability. The Minitab 17 software was used to check the significance of the developed models. In particular, each test involves nine passes of the workpiece, as shown in Table 9.

Table 9: Parameters according to the Taguchi Orthogonal Array design L9 (3^4) for Al-6% SiC -6% B_4C

No.	Con.%	V	Pon	Poff	MRR	TWR	SR
1	10	30	50	25	0.065	0.081	5.800
2	10	40	100	50	0.072	0.109	5.973
3	10	50	150	75	0.077	0.142	6.165
4	20	30	100	75	0.039	0.008	4.757
5	20	40	150	25	0.113	0.086	6.681
6	20	50	50	50	0.079	0.028	5.218
7	30	30	150	50	0.009	0.007	5.362
8	30	40	50	75	0.037	0.035	5.942
9	30	50	100	25	0.055	0.077	6.686

When the Pon value and the voltage increase, more discharge energy is released, thereby generating more heat. This leads to the melting and evaporation of the material particles as a form of (CuO) on the electrode surface, causing wear on the surface.

3.1 The Effect of machining on the MRR

Table 10 provides a detailed analysis of the effects of Pon, Poff, concentration, and voltage on the material removal rate (MRR) for the Al-6%SiC-6%B_4C compositematerial. The results indicate that increasing Pon from 50 to 150 µs at a concentration of 10% led to an 18.46% increase in the MRR. Furthermore, the table highlights that the optimum MRR of 0.113 g/min was achieved under operating conditions of 40 V, 150 µs Pon, and 25 µs Poff. These findings demonstrate that an increase in voltage and Pon significantly enhances the MRR. Additionally, at a concentration of 30%, an increase in voltage and Pon from 50 to 100 µs resulted in 48.65%improvement in the MRR [31]. Figure 8 illustrates the impact of Ton, Toff, voltage, and concentration on the MRR for the studied composite material. The Taguchi analysis was performed to evaluate the MRR (g/min) concentration, voltage, Pon, and Poff, using the Al-6%SiC-6%B_4C composite as the workpiece. The

statistical results from the analysis of variance (ANOVA) are presented in Table 10. The F-ratio indicates the significance of each factor in the experiment, while the P-values determine the statistical relevance of these factors on the response. Table 11 provides the model summary, which evaluates the performance and reliability of the regression model used to predict the material removal rate (MRR). The summary includes key metrics such as the R-squared, adjusted R-squared, and the standard error of the regression. These metrics are essential for assessing how well the model fits the experimental data and its predictive accuracy, and the regression equation is provided in Equation 3.

Table 10: The Variance Analysis (ANOVA)

Source	DF	Adj ss	Adj ms	F- Value	P- Value
model	5	0.006514	0.001303	5.53	0.095
Linear	4	0.006498	0.001624	6.90	0.072
Con.%	1	0.003776	0.003776	16.04	0.028
Voltage	1	0.001601	0.001601	6.80	0.080
Pon	1	0.000054	0.000054	0.23	0.665
Poff	1	0.001067	0.001067	4.53	0.123
2- way interaction	1	0.001664	0.001664	7.07	0.076
Pon×Poff	1	0.001664	0.001664	7.07	0.076
Error	3	0.000706	0.000235		
Total	8	0.007220			

Table 10 presents the analysis of variance for the Material Removal Rate (MRR), indicating which factors significantly affect the machining process. P-Value: Measures the statistical significance of each factor. A smaller value (<0.05) suggests that the factor significantly impacts MRR. F-Value: Represents the ratio of variance explained by a factor to the variance due to error. A higher value indicates a stronger influence on the response variable. Adjusted Mean Square (Adj ms) and Adjusted Sum of Squares (Adj ss): Reflect the contribution of each factor to the total variance. Degrees of Freedom (DF): Indicates the number of independent values or levels for each factor. The P-value (0.028) and a high F-value (16.04) indicate that it significantly affects MRR. This is due to its direct influence on electrochemical reactions and discharge energy available for material removal. A P-value of 0.080 and an F-value of 6.80 suggest moderate significance. Increasing voltage increases discharge energy, improving MRR but with diminishing returns at higher levels. Pulse-on time (Pon) and Pulse-off time (Poff): Both factors have P-values > 0.05, suggesting lower individual significance. However, their interaction (Pon × Poff) shows some impact (P-value: 0.076). The small Adj ss value for error indicates minimal unexplained variance, reflecting a robust model. Table 11 summarizes the goodness-of-fit metrics for the regression model used to predict MRR. R-squared (R-sq): Indicates the percentage of variance in MRR explained by the model. A value of 90.22% means the model captures most of the variation, suggesting high reliability. Adjusted R-squared (R-sq adj): Adjusted for the number of predictors, it remains high at 73.91%, confirming the model's validity. Predicted R-squared (R-sq pred): At 0.00%, this low value suggests the model might not generalize well to unseen data, possibly due to overfitting or limitations in the dataset. In the discussion of results, concentration directly affects the ion density in the electrolyte, facilitating more effective electrochemical reactions. Higher concentrations enhance the material removal but can lead to heat accumulation, potentially causing tool wear or surface roughness issues. Increasing voltage raises the energy delivered per discharge, increasing MRR. However, excessive voltage can create instability, such as arc formation, leading to inconsistent removal rates and degraded surface quality. Longer pulse-on times allow more energy to be delivered, aiding in material removal. However, excessively high Pon can cause overheating, leading to re-deposition or material vaporization rather than efficient removal. Longer pulse-off times provide cooling periods, which stabilize the machining process. Short Poff intervals, while efficient for MRR, may increase the risk of thermal damage or tool wear. The interplay between Pon and Poff shows that balancing these factors is crucial. Excessive energy delivery during Pon, without adequate cooling during Poff, can lead to diminished returns in MRR and surface defects. While the high R-squared indicates a good fit for the experimental data, the low predicted R-squared suggests overfitting.

MRR increases with higher electrolyte concentration, reaching a peak at 20% before plateauing or slightly decreasing at 30%. Higher concentrations improve ion conductivity, facilitating more efficient electrochemical reactions. However, excessive concentration can cause instability in the discharge process.MRR rises with increasing voltage as higher energy levels enhance material removal. The trend stabilizes or slightly declines beyond an optimal point due to factors like excessive heat and potential arcing, which can hinder effective material removal. Increasing Pon positively affects MRR, as longer discharges provide more energy for machining. However, excessively high Pon can lead to overheating, reducing machining efficiency, which decreases with longer Poff as extended cooling periods reduce the overall energy delivery per cycle, slowing the removal rate.

Equation 3 represents the regression equation:

$$MRR = -0.0237 - 0.003173\,X1 + 0.001633X2 + 0.001092X3 + 0.001531X4 - 0.000021X3 \times X4 \quad (3)$$

where Parameters: X1: Electrolyte concentration (%), X2: Voltage (V), X3: Pulse-on time (µs), X4: Pulse-off time (µs).

Table 11: The model summary

S	R-sq	R-sq (adj)	R-sq (pred)
0.0153449	90.22%	73.91%	0.00%

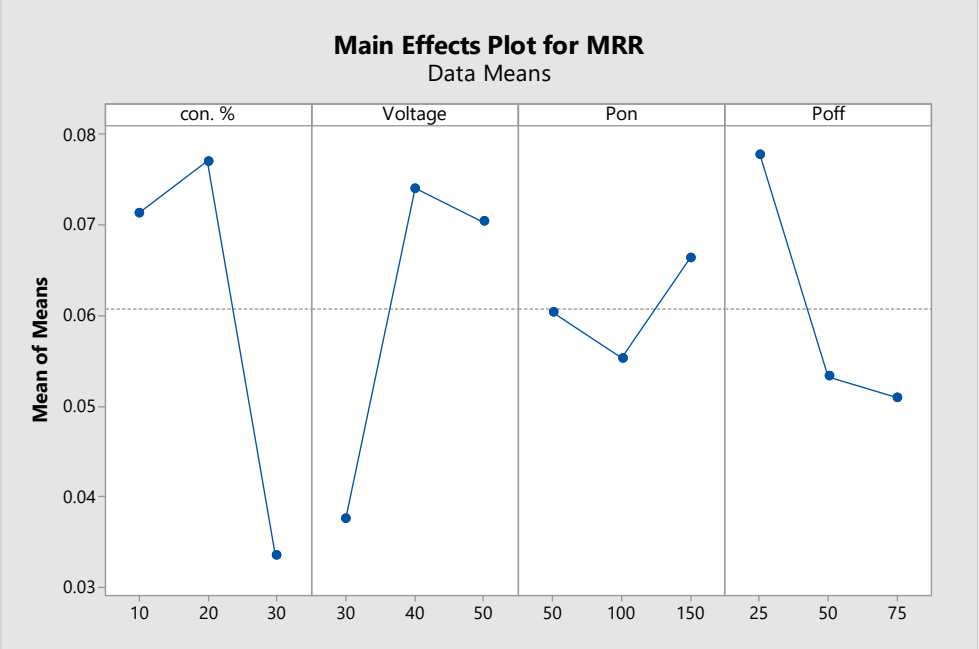

Figure 8: The effect plot of Ton, Toff, voltage, and concentration on MRR of the Al-6%SiC-6%B_4C composite material

3.2 The Effect of Machining on the TWR

The optimum TWR was achieved at 30% con., 30v, 150µsec Pon, and 50 µsec Poff. Particularly, increased concentration and reduced voltage were used to achieve the optimum TWR because the lower voltage ensures a controlled MRR and reduces the thermal impact on the tool. Figure 9 shows the effect plot of Ton, Toff, voltage, and concentration on the MRR of the Al-6%SiC-6%B_4C composite material. The Taguchi analysis includes the TWR (g/min) versus concentration, voltage, Pon, and Poff using the Al-6%SiC-6%B_4C as a workpiece. The analysis of variance (ANOVA), presented in Table 12, identifies the statistical significance of each factor—concentration, voltage, Pon, and Poffon the tool wear rate (TWR). The ANOVA results include key metrics such as the F-ratio, which indicates the relative importance of each factor, and the P-value, which determines whether a factor has a statistically significant effect on the TWR. Factors with a P-value below 0.05 are considered significant contributors to the response. The model summary, provided in Table 13, evaluates the regression model's accuracy and reliability in predicting the TWR. Metrics such as R-squared, adjusted R-squared, and the standard error of the regression are included to assess how well the model fits the experimental data. A high R-squared value suggests that the selected factors explain a large portion of the variability in the TWR, while a low standard error indicates precise predictions. These results validate the effectiveness of the regression model and highlight the key factors influencing the TWR, while the regression equation is shown in Equation 4.

Table 12: The variance analysis (ANOVA)

Source	DF	Adj ss	Adj ms	F- Value	P- Value
model	6	0.017566	0.002928	975.89	0.001
Linear	3	0.005761	0.001920	640.06	0.002
Voltage	1	0.003800	0.003800	1266.72	0.001
Pon	1	0.001380	0.001380	460.06	0.002
Poff	1	0.000580	0.000580	193.39	0.005
square	2	0.002969	0.001485	494.92	0.002
Voltage × Voltage	1	0.000760	0.000760	253.50	0.004
Poff×Poff	1	0.002209	0.002209	736.33	0.001
2-Way Interaction	1	0.009940	0.009940	3313.50	0.000
Voltage × Pon	1	0.009940	0.009940	3313.50	0.000
Error	2	0.000006	0.000003		
Total	8	0.017572			

This table presents the analysis of variance (ANOVA) for the Tool Wear Rate (TWR). It evaluates the significance of machining parameters and their interactions on the TWR using statistical metrics such as P-values, F-values, Adjusted Mean Square (Adj ms), and Adjusted Sum of Squares (Adj ss). P-Value: Determines statistical significance. A value <0.05 indicates

a strong influence of a parameter on TWR. F-Value: Indicates the magnitude of impact. Higher F-values show a stronger effect on the response variable. Adj ms and Adj ss: Reflect the variance explained by each parameter. Degrees of Freedom (DF): Denotes the levels of variation available for each parameter. The discussion of the result shows that Voltage is the most influential parameter affecting TWR. Higher voltage increases ion mobility and discharge energy, resulting in faster material removal but at the expense of higher tool wear due to thermal stress and oxidation. Longer Pon leads to more sustained energy application, increasing the removal rate but simultaneously exacerbating wear through continuous exposure to high temperatures. The impact of Pon demonstrates the importance of a balanced cooling period. Short Pon minimizes idle time and enhances productivity but increases thermal load and accelerates wear. Conversely, overly long Poff reduces productivity without proportional benefits to tool life. The square effects of voltage and Pon indicate that TWR does not increase linearly with these parameters. Extreme values lead to diminishing returns or adverse effects, such as material sticking or uneven wear. The significant interaction between voltage and Pon underscores the synergistic effects of increased energy levels and exposure time. This relationship highlights the need for careful balancing to optimize tool life without compromising productivity.

Table 13: The model summary

S	R-Sq	R-Sq (adj)	R-Sq (pred)
0.0017321	99.97%	99.86%	98.64%

This Table summarizes the goodness-of-fit metrics for the regression model used to predict Tool Wear Rate (TWR). It evaluates the model's ability to explain the variability in TWR based on machining parameters (voltage, electrolyte concentration, Pon, and Poff.

R-Sq (R-Squared): Represents the percentage of variation in TWR explained by the regression model. Value: 99.97% — The model explains almost all the variability in TWR, indicating an excellent fit. R-Sq Adj (Adjusted R-Squared): Adjusted for the number of predictors in the model, ensuring no overestimation of explanatory power. Value: 99.86% — Confirms the reliability of the model even after accounting for complexity. R-Sq Pred (Predicted R-Squared): Indicates how well the model predicts new data. Value: 98.64% — Demonstrates excellent predictive capability, validating the model's practical application.S (Standard Error of the Regression): Measures the average distance between observed and predicted values.Value: 0.0017321 — A very low value, confirming high precision in predictions.

The parameters studied voltage, Pon, Poff, and concentration have a direct and measurable impact on TWR, leading to a clear relationship. The inclusion of interaction terms (e.g., Voltage × Pon) captures the synergistic effects of multiple parameters, improving the model's explanatory power. The model's high R-Sq Pred value suggests that it can effectively guide process optimization, ensuring minimal tool wear under various conditions. This predictive capability is crucial for reducing costs and improving tool life in industrial applications. The low standard error implies that even small changes in machining parameters result in predictable variations in TWR. This sensitivity highlights the importance of precise parameter control during the machining process. While high Pon and voltage enhance material removal, they significantly increase TWR due to prolonged energy exposure. Introducing adequate Poff periods and moderating voltage can offset this effect, as reflected in the model's ability to predict optimal settings.

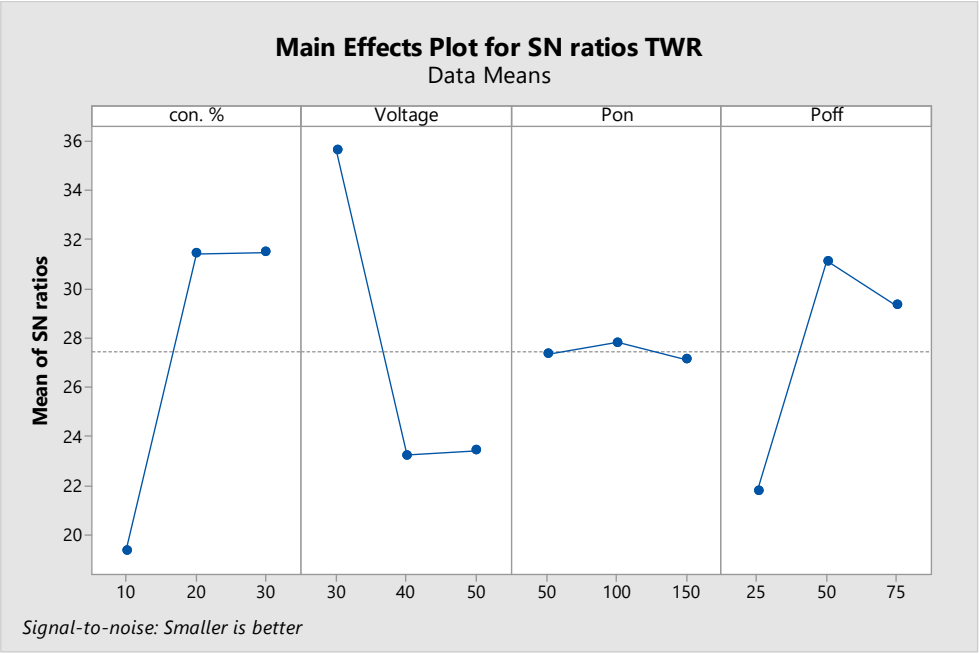

Figure 9: The effect plot of Ton, Toff, voltage, and concentration on MRR of the Al-6%SiC-6%B_4C composite material

This figure illustrates how the machining parameters Pon, Poff, Voltage, and Electrolyte Concentration) influence the Tool Wear Rate (TWR). Each curve shows the variation in TWR as the level of one parameter changes while holding others constant. TWR decreases with higher concentrations, stabilizing at 30%. This reduction occurs because increased ion availability improves energy efficiency, reducing unnecessary thermal load on the tool. TWR initially decreases with low to moderate voltage but starts increasing at higher values. Excessive voltage leads to intensified discharge energy, causing more tool wear due to thermal effects and oxidation. Longer Pon significantly increases TWR. Prolonged energy application raises the thermal stress on the tool, accelerating wear and degradation. TWR decreases as Poff increases. Longer cooling periods reduce thermal buildup, protecting the tool from excessive wear. However, overly long Poff can limit productivity by reducing overall machining efficiency.

Equation 4 represents the regression equation:

$$TWR = 0.0607 + 0.00402X2 - 0.005337X3 + 0.007127X4 - 0.000195X2 \times X2 - 0.000075X4 + 0.000141X2 \times X3 \quad (4)$$

3.3 The effect of machining on the SR

The optimum SR was achieved at 20% Con. 30v, 100 µsec Pon, and 75 µsec Poff because at a low voltage, the machining minimizes excessive energy and reduces micro-cracks formation. This combination of parameters creates stable machining, which reduces the SR by ensuring controlled energy application and material removal rate. Figure 10 shows the effect plot of Ton, Toff, voltage, and concentration on the MRR of the Al-6%SiC-6%B_4C composite material. The Taguchi analysis includes the SR (µm) versus concentration, voltage, Pon, and Poff using the Al-6%SiC-6%B_4C as a workpiece. The analysis of variance (ANOVA), presented in Table 14, evaluates the statistical significance of the factors—concentration, voltage, Pon, and Poff on the surface roughness (SR). The ANOVA results highlight metrics such as the F-ratio, which indicates the importance of each factor, and the P-value, which determines whether the factor has a statistically significant effect on the SR. Factors with a P-value below 0.05 are identified as having a significant influence on the response. The model summary, shown in Table 15, assesses the accuracy and reliability of the regression model in predicting SR. Metrics such as R-squared, adjusted R-squared, and standard error of the regression are included to measure the model's performance. A high R-squared value demonstrates that the independent variables effectively explain the variability in SR, while a low standard error reflects precise and consistent predictions. These metrics confirm the robustness of the model in identifying the key parameters affecting SR, and the regression equation is illustrated in Equation 5.

This table presents the ANOVA results for the Surface Roughness (SR), identifying the machining parameters and interactions that significantly influence SR. Determines the statistical significance of each parameter or interaction. A P-value < 0.05 indicates a significant effect on SR. Measures the strength of each factor's impact. Higher values indicate a more substantial effect on the response variable (SR). Adjusted Mean Square (Adj ms) and Adjusted Sum of Squares (Adj ss) reflect the contribution of each parameter to the total variance. Degrees of Freedom (DF): Represents the levels of variability for each factor. P-Value: 0.223 (not significant individually). Concentration alone does not have a major direct impact on SR, but its effects become significant when interacting with other parameters. P-Value: 0.073 (marginal significance). Voltage contributes moderately to SR, as higher energy levels can cause surface defects like micro-cracks due to excessive heat. P-Value: 0.013 (significant). Longer Pon increases SR by creating more thermal stress, leading to surface irregularities and micro-cracks. P-Value: 0.004 (highly significant). Adequate Poff reduces SR by providing cooling time, preventing thermal damage, and ensuring smoother surfaces. The small error term (P-value: 0.00006) confirms the robustness of the model, with most variability captured by the studied factors.

Table 14: The variance analysis (ANOVA)

Source	DF	Adj ss	Adj ms	F- Value	P- Value
model	7	3.34645	0.47806	7945.66	0.009
Linear	4	2.53988	0.63497	10553.52	0.007
Con.%	1	0.00045	0.00045	7.49	0.223
Voltage	1	0.00045	0.00459	76.26	0.073
Pon	1	0.13607	0.13607	2261.52	0.013
Poff	1	1.50743	1.50743	25054.18	0.004
Square	1	0.38019	0.38019	6318.98	0.008
Con.%×Con.%	1	0.38019	0.38019	6318.98	0.008
2-Way Interaction	2	1.05184	0.52592	8741.02	0.008
Con.% × Pon	1	0.70374	0.70374	11696.45	0.006
Con.% × Poff	1	0.00837	0.00837	139.18	0.054
Error	1	0.00006	0.00006		
Total	8	3.34651			

Table 15: The model summary

S	R-Sq	R-Sq (adj)	R-Sq (pred)
0.0077567	100.00%	99.99%	*

In this Table, R-Sq (R-Squared) 100.00% — The model explains all variability in SR, indicating a perfect fit for the experimental data. R-Sq Adj (Adjusted R-Squared):99.99% Reflects the model's reliability even after accounting for complexity, confirming minimal overfitting. R-Sq Pred (Predicted R-Squared):99.99%. The model demonstrates exceptional predictive capability, ensuring accuracy for unseen data. S (Standard Error of the Regression):0.0077567 — A very low standard error confirms high precision in SR predictions. Prolonged Pon increases energy application, which, while enhancing material removal, creates localized heating. This causes surface imperfections such as micro-cracks or re-deposition, degrading SR. Sufficient Poff intervals allow cooling, reducing thermal stress and ensuring a smoother surface. Insufficient cooling leads to defects, while excessive cooling can reduce productivity. Higher voltage introduces more energy into the system. While this aids material removal, excessive energy can cause surface damage due to localized melting. Concentration affects ion mobility and discharge stability. Moderate levels optimize energy efficiency, while extremes introduce inconsistencies, slightly impacting SR. The interaction between Concentration and Pon highlights the compounded effects of prolonged energy application with varying ion densities. This explains the significant impact on SR, as these parameters jointly influence discharge consistency and thermal effects. The interaction between Concentration and Poff emphasizes the importance of balancing ion density and cooling periods to optimize surface smoothness. With perfect R-squared values (R-Sq and R-Sq Pred), the model is not only an excellent fit for the observed data but also highly reliable for predicting SR in other scenarios. The extremely low standard error reinforces this precision.

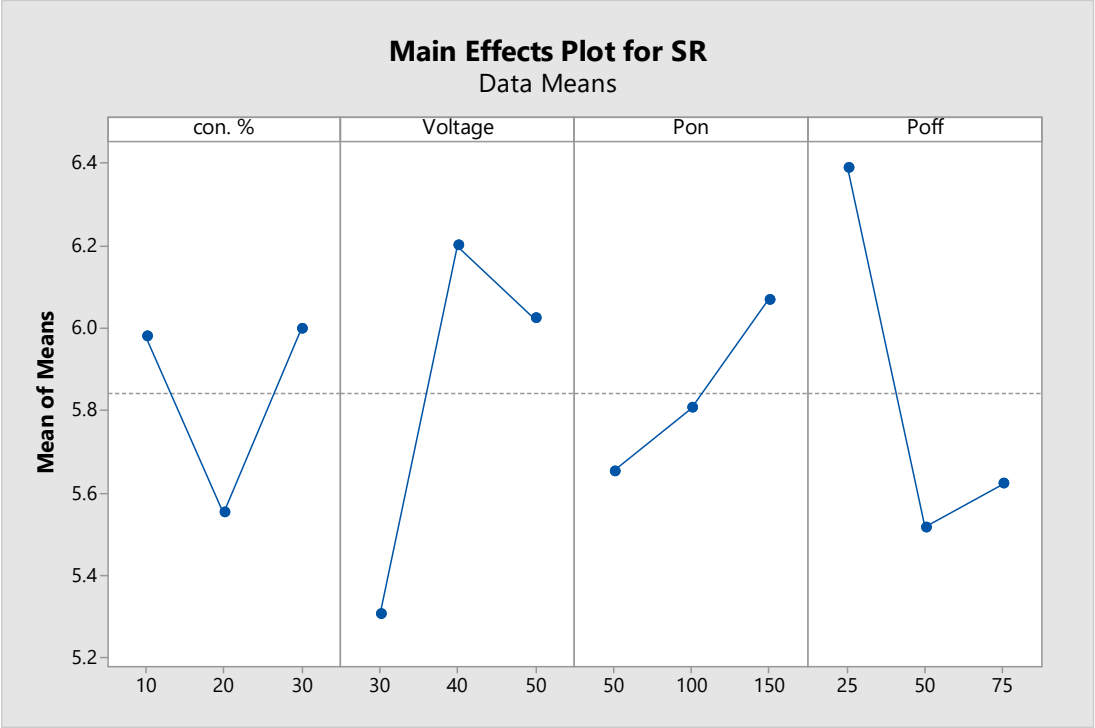

Figure 10: The effect plot of Ton, Toff, voltage, and concentration on the MRR of the Al-6%SiC-6%B_4C composite material

This figure illustrates the relationship between the machining parameters Pon, Poff, Voltage, and Electrolyte Concentration) and their impact on Surface Roughness (SR). Each curve represents how SR changes as one parameter varies while others are held constant.SR improves (decreases) with an increase in concentration up to 20%. This is due to better ion conductivity, stabilizing discharge, and reducing surface defects. Beyond 20%, SR slightly worsens due to potential instability or uneven energy distribution.SR worsens as voltage increases. Higher voltage leads to excessive discharge energy, causing surface damage such as micro-cracks and material melting.SR increases with longer Pon. Prolonged energy application introduces localized overheating, degrading the surface finish.SR improves with longer Poff as adequate cooling intervals prevent thermal damage and ensure a smoother surface. However, excessively long off can marginally reduce productivity without significantly enhancing SR. Equation 5 represents the regression equation:

$$SR = 5.3340 - 0.00093X1 - 0.007317X2 + 0.043963X3 - 0.043180X4 + 0.004360X1 \times X1 - 0.001937X1 \times X3 + 0.000423X1 \times X4 \quad (5)$$

The combination of Figure 8 and Equation 5 provides a comprehensive understanding of how to optimize SR. Industries can use this model to predict and fine-tune parameters to achieve smooth finishes. Table 16 compares this research with previous research.

Table 16: Comparison the results of current work with that reported in the literature

Study	Goals	Methodology	Key Findings	Similarities to This Study	Differences from This Study
Yan et al. (2021) [9]	Investigate process parameters for high SiC-content composites in wire EDM.	DOE and ANOVA for parameter effects.	High Ton increases MRR; excessive Toff reduces efficiency.	Analyzed Ton and Toff effects on machining.	Focused on wire EDM; and different composite types.
Abbas et al. (2022) [10]	Optimize ECM parameters for aluminum MMCs using Taguchi methods.	Taguchi optimization of ECM variables.	Higher energy discharge improves MRR but degrades SR.	Optimized parameters with Taguchi methods.	Did not emphasize balancing MRR and SR.
Gugulothu et al. (2021) [12]	Study ECM parameters on MRR of Al5086/SiC/Fly Ash composites.	Statistical analysis of ECM parameters.	MRR decreases slightly with higher electrolyte concentration.	Studied MRR in hybrid composites.	Focused on feed rate; not explored in this study.
Mandal et al. (2022) [13]	Analyze micro-ECDM and powder-mixed ECDM on MRR and SR.	Box-Behnken design and powder additives.	PMECDM improves MRR and reduces SR over µ-ECDM.	Focus on enhancing both MRR and SR.	Introduced powder additives for machining.
Selvarasu et al. (2023) [15]	Optimize EDM for AZ61/7.5% B_4C composites with nano SiC oil.	Taguchi-based analysis with nano SiC oil.	Nano SiC oil achieves 81% MRR, 55% EWR, and 47% SR improvement.	Optimization of EDM parameters for hybrid composites.	Used nano SiC oil; different dielectric medium.
Dusanapudi et al. (2023) [16]	Enhance die-sinking EDM for hybrid MMCs using stir-cast composites.	Experimental EDM parameter optimization.	Optimized Ton and current enhance MRR, TWR, and SR.	Studied Ton and current effects on machining performance.	Studied stir-cast composites and different materials.
Mohankumar et al. (2024) [17]	Optimize EDM parameters for Al7075/B_4C using hybrid optimization techniques.	Taguchi, EWM, TOPSIS, GRA hybrid optimization.	15% improvement in closeness coefficients and Grey grades.	Hybrid optimization for EDM parameters.	Applied hybrid optimization techniques; complex design.
Arif et al. (2024) [18]	Develop and validate a thermal model for EDM of hybrid composites.	Thermal modeling and experimental validation.	Pulse current, Ton, and SiC affect MRR and SR optimization.	Focus on parameter optimization for MRR and SR.	Focused on thermal modeling; not applied here.
Arunachalam et al. (2024) [19]	Study EDM parameters for MoS2/B_4C/AZ31 Mg alloy composites.	Powder metallurgy and EDM parameter testing.	Powder metallurgy enhances wear resistance and hardness.	Parameter optimization for composite machining.	Used powder metallurgy for composite enhancement.
This Study	Optimize ECDM parameters for Al6061/SiC/B_4C hybrid composites.	Taguchi and ANOVA for multi-parameter optimization.	Balanced optimization of MRR (0.113 g/min) and SR (5.218 µm).	Multi-parameter optimization for hybrid composites.	Focused on ECDM for balanced MRR and SR optimization.

4. Conclusion

This study demonstrated the effectiveness of the ECDM process in machining hybrid composite materials. Optimizing machining parameters significantly improved material removal rate (MRR), tool wear rate (TWR), and surface roughness (SR).

The optimal MRR achieved was 0.113 g/min under the conditions of 20% electrolyte concentration, 40 V voltage, 150 µs pulse-on time, and 25 µs pulse-off time. The MRR increased by 18.46% at higher pulse-on durations and electrolyte concentrations, showcasing enhanced productivity. The minimum TWR recorded was 0.007 g/min, achieved at 30% electrolyte concentration, 30 V voltage, 150µs pulse-on time, and 50µs pulse-off time. In this regard, the controlled use of the lower voltage and the optimized electrolyte concentration reduced the thermal impact on the tool, enhancing its lifespan. The

best surface quality, represented by an SR of 4.757 µm, was observed under the conditions of 20% electrolyte concentration, 30 V voltage, 100µs pulse-on time, and 75µs pulse-off time. These results confirmed the feasibility of ECDM for machining high-hardness hybrid composites. The study provided a practical framework for optimizing machining productivity while maintaining precision. The insights gained can contribute to the advancement of machining technologies for hybrid composites in aerospace, automotive, and defense applications..

Author contributions

Conceptualization, **S. Lafta**. and **A. Ibrahim**; data curation, **S. Lafta**.; formal analysis, **S. Lafta**.; investigation, **S. Lafta**.; methodology,**S. Lafta**. and **A. Ibrahim** .; project administration, **A. Ibrahim**, resources,**S. Lafta**. and **A. Ibrahim** .; software, **S. Lafta** .; supervision, **A. Ibrahim**.; validation, **S. Lafta**. and **A. Ibrahim** .; visualization, **S. Lafta**. and **A. Ibrahim** ; writing—original draft preparation, **S. Lafta**.; writing—review and editing, **A. Ibrahim**. All authors have read and agreed to the published version of the manuscript.

Funding

This research received no specific grant from any funding agency in the public, commercial, or not-for-profit sectors.

Data availability statement

The data that support the findings of this study are available on request from the corresponding author.

Conflicts of interest

The authors declare that there is no conflict of interest.

References

[1] U. Ozmen and I. Asil Turk, Electrochemical discharge machining: A review, Int. J. Eng. Sci. Eng. Appl., 5 (2016) 495–499. https://doi.org/10.7753/IJSEA0510.1006

[2] K. K. Chawla, Composite materials, Sci. Eng. Springer Sci. Business Media, 13 (2012) 72. https://doi.org/10.1557/S088376940006379X

[3] B. Bhattacharyya and S. K. School, Investigation for controlling electrochemical machining through response surface methodology based approach, J. Mater. Process. Technol., 86 (1999) 200–207. https://doi.org/10.1016/S0924-0136(98)00311-2

[4] X. Ding, W.Y.H. Liew, and X.D. Liu, Evaluation of machining performance of MMC with PCBN and PCD tools wear, Wear, 259 (2005) 1225–1234. https://doi.org/10.1016/j.wear.2005.02.094

[5] X. M. Anthony and Ajitkumar, Machinability of hybrid metal matrix composite: A review, Procedia Eng., 174 (2017) 1110–1118. https://doi.org/10.1016/j.proeng.2017.01.264

[6] N. P. Hung, F. Y. C. Boey, and K. A. Khor, Machinability of cast and powder-formed aluminum alloys reinforced with SiC particles, J. Mater. Process. Technol., 48 (1995) 291–297. https://doi.org/10.1016/0924-0136(94)01661-J

[7] Y. Sumankant, C. S. Jawalkar, A. Singh Verma, and N. M. Surie, Fabrication of aluminum metal matrix composites with particulate reinforcement: A review, Mater. Today Proc., 4 (2017) 2927–2936. https://doi.org/10.1016/j.matpr.2017.02.174

[8] H. Kala, K. K. S. Mer, and S. Kumar, A review on mechanical and tribological behaviours of stir cast aluminum matrix composites, Procedia Mater. Sci., 6 (2014) 1951–1960. https://doi.org/10.1016/j.mspro.2014.07.229

[9] H. Yan, B.D. Kabongo, H. Zhou, C. Wu, and Z. Chen, Analysis and optimization of the machining characteristics of high-volume content SiCp/Al composite in wire electrical discharge machining, Crystals, 11 (2021) 1342. https://doi.org/10.3390/cryst11111342

[10] F. Abbas, S. M. Mousa, and D. A. Noori, Investigation and optimization of machining parameters in electrochemical machining of aluminum metal matrix composites, Period. Eng. Nat. Sci., 10 (2022) 48–59. https://doi.org/10.21533/pen.v10i3.3006

[11] F. Abbas, A. H. Singal, and D. A. Noori, Investigation of material removal rate and surface roughness during electrical discharge machining on Al (6061)-5%SiC-10%B4C hybrid composite, Metall. Mater. Eng., 28 (2022) 47–60. https://doi.org/10.30544/798

[12] B. Gugulothu, P.S. Satheesh Kumar, B. Srinivas, A. Ramakrishna, and S. Vijayakumar, Investigating the Material Removal Rate Parameters in ECM for Al 5086 Alloy-Reinforced Silicon Carbide/Flyash Hybrid Composites by Using Minitab-18, Adv. Mater. Sci. Eng., 2021 (2021) 1-6. https://doi.org/10.1155/2021/2079811

[13] N. Mandal, S. Hloch, and A. Kumar Das, Comparison of maraging steel surface integrity in hybrid and conventional micro-ECDM processes, Materials, 15 (2022) 4378. https://doi.org/10.3390/ma15134378

[14] N. Mandal, N. Kumar, and A. K. Das, Machining of maraging steel through Al_2O_3 abrasive powder-assisted electrochemical discharge machining, Adv. Modern Mach. Processes, (2022) 101–110. https://doi.org/10.1007/978-981-19-7150-1_9

[15] S. Selvarasu, M. Subramanian, and J. Thangasamy, An effect of nano-SiC with different dielectric mediums on AZ61/7.5% B4C nanocomposites studied through electrical discharge machining and Taguchi-based complex proportional assessment method, Matéria Rio de Janeiro, 28 (2023) e20230058. https://doi.org/10.1590/1517-7076-RMAT-2023-0058

[16] S. Dusanapudi and L. S. D. Lanka, An improvement of die sinking EDM using on hybrid metal matrix composites, Int. J. Sci. and Technol. Res., 9 (2023) 2413–2418.

[17] V. Mohankumar, S. Kapilan, A. Karthik, M. Bhuvaneshwaran, C. Santulli, D. T. Kumar, S. Palanisamy, and C. Fragassa, Hybrid design of experiment approach in analyzing the electrical discharge machining influence on stir cast Al7075/B4C metal matrix composites, Metals, 14 (2024) 205. https://doi.org/10.3390/met14020205

[18] U. Arif, I.A. Khan, and F. Hasan, Thermal modelling and parametric optimization for machining of aluminum (Al-10%SiCmicro-SiCnano) based hybrid composite using spark erosion, Aligarh Muslim University, 2023. https://doi.org/10.21203/rs.3.rs-3095363/v1

[19] J. Arunachalam, R. Saravanan, T. Sathish, E. Makki, and J. Giri, Influence of machining process of MoS2/B4C/AZ31 Mg alloy composite and its tribological characteristics, AIP Advances, 14 (2024) 035342. https://doi.org/10.1063/5.0200492

[20] V. Mohankumar, S. Prakash, K. Palanisamy, K. Mani, D.T. Kumar, M. Sillanpää, and S.A. Al-Farraj, Process parameters optimization of EDM for hybrid aluminum MMC using hybrid optimization technique, Heliyon, 10 (2024) e35555. https://doi.org/10.1016/j.heliyon.2024.e35555

[21] S.J. Ebeid, M.S. Hewidy, T.A. El-Taweel, and H. Youssef, Towards higher accuracy for ECM hybridized with low-frequency vibrations with response surface methodology, J. Mater. Process. Technol., 149 (2004) 432–438. https://doi.org/10.1016/j.jmatprotec.2003.10.046

[22] H. M. A. Mahmoud, P. Satishkumar, Y. Srinivasa Rao, R. Chebolu, R. Y. Capangpangan, A. C. Alguno, M. Gopal, A. Firos, and M.C. Saravana, Investigation of mechanical behavior and microstructure analysis of AA7075/SiC/B4C-based aluminum hybrid composites, Adv. Mater. Sci. Eng., 2022 (2022) 2411848. https://doi.org/10.1155/2022/2411848

[23] U. Farooq, H.A. Bhatti, M. Asad, M.S. Kumar, S. Zahoor, and A.M. Khan, Surface generation on titanium alloy through powder-mixed electric discharge machining with the focus on bioimplant applications, Int. J. Adv. Manuf. Technol., 122 (2022) 1395–1411. https://doi.org/10.1007/s00170-022-09927-1

[24] V. Rajput, M. Goud, and N.M. Suri, Electrochemical discharge machining: Gas film electrochemical aspects, stability parameters, and research work, J. Electrochem. Soc., 168 (2021) 013503. https://doi.org/10.1149/1945-7111/abd516

[25] B. Mazza, P. Pedeferri, and G. Re, ‘‘Hydrodynamic instabilities in electrolytic gas evolution, Electrochimica Acta, 23 (1978) 87–93. https://doi.org/10.1016/0013-4686(78)80102-9

[26] R. Wüthrich, U. Spaelter, and H. Bleuler, The current signal in spark-assisted chemical engraving (SACE): What does it tell us? J. Micromech. Microeng., 16 (2006) 779. https://doi.org/10.1088/0960-1317/16/4/014

[27] R. Wüthrich and L.A. Hof, The gas film in spark-assisted chemical engraving (SACE)—A key element for micro-machining applications, Int. J. Mach. Tools Manuf., 46 (2006) 828–835. https://doi.org/10.1016/j.ijmachtools.2005.07.029

[28] A. Bin Sapit, S.K. Shather, and F.N. Abed, Enhancement of the performance surface roughness of wire cutting process by additives nano [Al_2O_3], Period. Eng. Nat. Sci., 8 (2020) 933–941. https://doi.org/10.21533/pen.v8i4.1627

[29] M. Hourmand, A.A. Sarhan, S. Farahany, and M. Sayuti, Microstructure characterization and maximization of the material removal rate in nano-powder mixed EDM of Al-Mg2Si metal matrix composite ANFIS and RSM approaches, Int. J. Adv. Manuf. Technol., 101 (2019) 2723–2737. https://doi.org/10.1007/s00170-018-3130-3

[30] N.K. Singh, P.M. Pandey, and K.K. Singh, Experimental investigations into the performance of EDM using argon gas-assisted perforated electrodes, Mater. Manuf. Processes, 32 (2017) 940–951. https://doi.org/10.1080/10426914.2016.1221079

[31] M.H. Jokhio, P.M. Ibrahim, and M.A. Unar, Manufacturing of aluminum composite material using stir casting process, Mehran University Res. J. Eng. Technol., 30 (2016) 37–40. https://doi.org/10.48550/arXiv.1604.01251